(10) Martire, D. E.; Riedl, P. *J. Phys. Chem.* **1968**, *72*, 3478.
(11) DiPaola-Baranyi, G.; Guillet, J. E.; Jeberien, H. E.; Klein, J. *Makromol. Chem.* **1980**, *181*, 215.
(12) Dwyer, J.; Karim, K. A. *Ind. Eng. Chem. Fundam.* **1975**, *14*, 196.
(13) Karim, K. A.; Bonner, D. C. *J. Appl. Polym. Sci.* **1978**, *22*, 1277.
(14) Dincer, S.; Bonner, D. C. *Macromolecules* **1978**, *11*, 107.
(15) Galin, M. *Polymer*, in press.
(16) Riddick, J. A.; Bunger, W. B. "Organic Solvents" Organic Solvents"; Wiley-Interscience: New York, 1970.
(17) Welch, G. J. *Polymer* **1974**, *15*, 429.
(18) Galin, M. *Macromolecules* **1977**, *10*, 1239.
(19) Patterson, D.; Tewari, Y. B.; Schreiber, H. P.; Guillet, J. E. *Macromolecules* **1971**, *4*, 356.
(20) Dreisbach, R. R. *Adv. Chem. Ser.* **1955**, *No. 15*; **1959**, *No. 22*; **1961**, *No. 29*.
(21) Hong, C. S.; Wakslak, R.; Finston, H.; Fried, V. *J. Chem. Eng. Data* **1982**, *27*, 146.
(22) O'Connell, J. P.; Prausnitz, J. M. *Ind. Eng. Chem. Process. Des. Dev.* **1967**, *6*, 245.
(23) Olabisi, O. *J. Appl. Polym. Sci.* **1978**, *22*, 1021.
(24) McClellan, Tables of Experimental Dipole Moments"; Rahara Enterprises: El Cerrito, CA, 1974; Vol. 2.
(25) Kamlet, M. J.; Abboud, J. L.; Abraham, M. H.; Taft, R. W. *J. Org. Chem.* **1983**, *48*, 2877.
(26) DiPaola-Baranyi, G.; Fletcher, S. J.; Degre, P. *Macromolecules* **1982**, *15*, 885.
(27) Ehrenson, S. *J. Org. Chem.* **1979**, *44*, 1793.
(28) Krygowski, T. M.; Fawcett, W. R. *J. Am. Chem. Soc.* **1975**, *97*, 2143.
(29) Alley, S. K.; Scott, R. L. *J. Phys. Chem.* **1963**, *67*, 1182.
(30) Marriott, S.; Reynolds, W. F.; Taft, R. W.; Topson, R. D. *J. Org. Chem.* **1984**, *49*, 959.
(31) Garton, A.; Cousin, P.; Prud'homme, R. E. *J. Polym. Sci., Polym. Phys. Ed.* **1983**, *21*, 2275.
(32) Fowkes, F. M.; Tischler, D. O.; Wolfe, J. A.; Lannigan, L. A.; Ademu-John, C. M. *J. Polym. Sci., Polym. Chem. Ed.* **1984**, *22*, 547.
(33) Chapman, N. B.; Shorter J. "Correlation Analysis in Chemistry"; Plenum Press: New York and London, 1978.
(34) Krygowski, T. M.; Milczarek, E.; Wrona, P. K. *J. Chem. Soc. Perkin Trans. 2* **1980**, 1563.
(35) Olabisi, O.; Robeson, L. M.; Shaw, M. T. "Polymer-Polymer Miscibility"; Academic Press: New York, 1979.
(36) Galin, M. *Makromol. Chem., Rapid Commun.* **1984**, *5*, 119.
(37) Paul, D. R.; Barlow, J. W.; Bernstein, R. E.; Wahrmund, D. C. *Polym. Eng. Sci.* **1978**, *18*, 1225.
(38) Roerdink, E.; Challa, G. *Polymer* **1980**, *21*, 509.
(39) Hansen, C. M. *J. Paint Technol.* **1967**, *39*, 104.
(40) Shimidzu, T.; Yoshikawa, M. *Polym. J. (Tokyo)* **1983**, *15*, 135.
(41) Law, K. Y.; Loutfy, R. O. *Polymer* **1983**, *24*, 439.

Inverse Gas Chromatography. 3. Dependence of Retention Volume on the Amount of Probe Injected

Petr Munk,* Zeki Y. Al-Saigh, and Timothy W. Card

Department of Chemistry and Center for Polymer Research, University of Texas at Austin, Austin, Texas 78712. *Received December 11, 1984*

ABSTRACT: A theory is developed for studying the effect of probe concentration on the chromatographic behavior of inverse gas chromatography (IGC) columns. The dependence of retention volume of the probe on the volume of probe injected is linear in the range of routine injections. The slope of the dependence is a function of the reduced retention volume and of the ratio of retention volume and the width of the peak. The theory does not introduce any adjustable parameters. The theory described well the experimental data obtained on three columns loaded with different amounts of polyisobutylene; three flow rates and three alkane probes were used at two different temperatures. The theory allows one to estimate from a single IGC experiment the correction needed for obtaining retention volumes extrapolated to the vanishing concentration of the probe.

In our on-going research on inverse gas chromatography (IGC), we have been trying to improve the experimental precision of the method by developing a new coating technique,[1] by improving the measurement of the flow rate,[2] and by correcting the data for the interaction of the probe with the chromatographic support.[3] In this paper, we will analyze, theoretically and experimentally, the dependence of retention volumes on the amount of the injected probe. Polyisobutylene was used as a model polymer; it has already been studied by a number of researchers.[4-11] Leung and Eichinger[4] have reported, but not analyzed, the dependence of retention volume on the size of the injection.

Theory

Let us assume that the effect of the chromatographic support has been corrected for. Then the retention volume of the probe is related to the distribution coefficient of the probe between the gas phase and the polymer phase. The distribution coefficient is generally concentration-dependent. We will now calculate this dependence using the Flory-Huggins theory of polymer solutions with a constant value of the well-known parameter χ.

In the following, we will use subscript 1 for the probe, subscript 2 for the polymer, superscript l for the liquid phase, and superscript g for the gas phase; c is concentration (g/mL). The Flory-Huggins relation for the change of the Gibbs function in the process of mixing, ΔG_{mix}, reads

$$\Delta G_{mix} = RT[n_1^l \ln \phi_1^l + n_2^l \ln \phi_2^l + n_1^l \phi_2^l \chi] \quad (1)$$

where n_i and ϕ_i are the number of moles and volume fraction of the ith component, respectively; RT has its usual meaning. Concentration c_1^l is related to the volume fraction as $\phi_1^l = v_1^l c_1^l$, where v_1^l is the specific volume of the probe.

At equilibrium, the difference $\Delta\mu_1$ of the chemical potential of the probe in either phase from the chemical potential in the reference state (pure probe, temperature of the column T, saturated vapor pressure P_1^0 at this temperature) is the same $\Delta\mu_1^l = \Delta\mu_1^g$. A routine thermodynamic treatment yields

$$RT \ln (RTc_1^g/M_1P_1^0) - (B_{11} - V_1^l)P_1^0 = (\partial\Delta G_{mix}/\partial n_1^l)_{n_{j\neq1},P,T} \quad (2)$$

where P_1^0 and M_1 are the saturated vapor pressure and molecular weight of the probe, respectively, V_i^l is the molar volume of the ith component, and B_{11} is the second virial coefficient of the probe in the gas phase.

Combination of eq 1 and 2 yields after some rearrangements

0024-9297/85/2218-2196$01.50/0

$$\ln (c_1^g/c_1^l) = \ln (V_1^l P_1^0/RT) + 1 - (V_1^l/V_2^l) + \chi + (B_{11} - V_1^l)P_1^0/RT - c_1^l v_1^l[1 - (V_1^l/V_2^l) + 2\chi] + (c_1^l v_1^l)^2\chi \quad (3)$$

Equation 3 represents the dependence of the partition coefficient c_1^l/c_1^g on the concentration of the probe in the polymer phase.

The retention volume of the probe V_r and the void volume of the column V_0 are defined in a usual way as

$$V_r = (t_p - t_m)Fj \quad (4)$$

$$V_0 = t_m Fj \quad (5)$$

where F is the flow rate of the carrier gas measured at the outlet pressure and normalized to the column temperature, t_p and t_m are the retention times of the probe and the marker, respectively, $j \equiv 3(P^2 - 1)/2(P^3 - 1)$ is the correction factor for gas expansion on the column, and $P \equiv P_i/P_o$, where P_i and P_o are the inlet and outlet pressures, respectively.

Routine analysis of the transport of a probe on a chromatographic column shows that V_r is related to the partition coefficient as

$$V_r = (c_1^l/c_1^g)V_p \quad (6)$$

where $V_p = w_2 v_2$ is the volume of the polymer phase on the column, w_2 is the mass of the polymer on the column, and v_2 is its specific volume. Equation 6 was derived under the assumption that the partition coefficient is independent of the probe concentration and that the swelling of the polymer by the probe causes only negligible change of the volume of the polymeric phase.

When these assumptions are not fulfilled, eq 6 may still be applied provided that a movement of a probe zone of constant concentration through the column is considered. V_p is equal in this case to

$$V_p = w_2 v_2/\phi_2 \quad (7)$$

Combination of eq 3, 6, and 7 yields after rearrangement

$$\ln (w_2 v_2/V_r) = \ln (V_1^l P_1^0/RT) + 1 - V_1^l/V_2^l + \chi + (B_{11} - V_1^l)P_1^0/RT + \ln (1 - c_1^l v_1^l) - c_1^l v_1^l(1 - V_1^l/V_2^l + 2\chi) + (c_1^l v_1^l)^2\chi \quad (8)$$

In the limit of a vanishingly small amount of the injected probe, c_1^l is vanishingly small everywhere and at all times, and eq 8 reduces to the well-known expression

$$\ln (w_2 v_2/V_r^*) = \ln (V_1^l P_1^0/RT) + 1 - V_1^l/V_2^l + \chi + (B_{11} - V_1^l)P_1^0/RT \quad (9)$$

Here, the asterisk in V_r^* signifies a value corresponding to a vanishingly small injection. Combination of eq 8 and 9 yields

$$\ln (V_r/V_r^*) = c_1^l v_1^l(1 - V_1^l/V_2^l + 2\chi) - \ln (1 - c_1^l v_1^l) + (c_1^l v_1^l)^2\chi \quad (10)$$

For typical IGC experiments, the product $c_1^l v_1^l$ will be much smaller than unity; furthermore, the ratio V_1^l/V_2^l for high molecular weight polymers is negligible with respect to unity. Thus, the following expressions are good approximations:

$$V_r/V_r^* \approx \exp[2c_1^l v_1^l(1 + \chi)] \approx 1 + 2c_1^l v_1^l(1 + \chi) \quad (11)$$

Experimentally, c_1^l is a function of the position on the column and of the time after probe injection. In the following, we will use eq 11 for evaluation of actual experiments; we will calculate c_1^l as an appropriate space and time average.

In a typical chromatographic experiment, the concentration profile of the probe on the column is Gaussian and its characteristic parameter, σ, is increasing as the probe travels along the column. In the following calculation we will neglect the effects of the changing pressure along the column. Then the peak will travel along the column with a constant velocity. Due to the peak spreading within the plumbing, the characteristic parameter will have a value σ_i at the inlet of the column, its value at the outlet (equal to the value at the detector) will be $\sigma_o = \sigma_{det}$. Then the time-dependent value of σ is given as

$$\sigma^2 = \sigma_i^2 + (\sigma_o^2 - \sigma_i^2)x_{max}/l \quad (12)$$

Here, the length coordinate of the column is denoted as x, the length of the column is l, and the time-dependent position of the peak maximum is x_{max}.

The experimentally known quantities include the mass of the polymer in the column w_2, the volume V_{inj} and specific volume v_1^l of the injected probe, the retention volume of the probe V_r, the void volume V_0, and the width $V_{h/2}$ at the half-height of the peak reaching the detector. The width $V_{h/2}$ is expressed in units of volume of the carrier gas; it is measured at the detector. The width is related to other parameters as

$$V_{h/2} = V_{tot}(\sigma_o/l)[2(\ln 2)^{1/2}] \quad (13)$$

where $V_{tot} \equiv V_0 + V_r$.

Finally, the amount of probe dm_1 in a volume element of the column of the length dx is given by

$$dm_1 = A \exp[-((x - x_{max})/\sigma)^2]\, dx \quad (14)$$

where the time-dependent factor A follows from the law of mass conservation: the mass of the probe on the column is equal to the mass injected V_{inj}/v_1^l. Thus

$$V_{inj}/v_1^l = \int_0^l dm_1 \approx \int_{-\infty}^{+\infty} dm_1 = A\sigma\pi^{1/2} \quad (15)$$

Let us now calculate c_1^l and c_1^g as a function of x. The volume element of the column contains void volume $dV_0 = (V_0/l)\, dx$ and polymer volume $dV_p = (w_2 v_2/l)\, dx$. Obviously

$$dm_1 = c_1^g\, dV_0 + c_1^l\, dV_p \quad (16)$$

or using eq 14 and 15

$$\frac{V_{inj}}{v_1^l \sigma\pi^{1/2}} \exp\left[-\left(\frac{x - x_{max}}{\sigma}\right)^2\right] = \frac{c_1^g V_0}{l} + \frac{c_1^l w_2 v_2}{l} \quad (17)$$

Substituting for c_1^g from eq 6, we obtain after some manipulation

$$c_1^l = \frac{l V_{inj} V_r}{v_1^l w_2 v_2 \sigma\pi^{1/2} V_{tot}} \exp[-((x - x_{max})/\sigma)^2] \quad (18)$$

In our approximation, the probe peak will move along the column as if the distribution coefficient had the same value everywhere within the peak; the value should correspond to the average concentration of $\bar{c}_1^l$ within the peak. The appropriate average (applicable to most transport processes) is the mass-weighted average. Accordingly, the average concentration of the peak (which is still a function of the position of the peak on the column and through it of time t) may be written as

$$c_1^l(t) = \int_0^l c_1^{l\,2}\, dx / \int_0^l c_1^l\, dx \approx \int_{-\infty}^{+\infty} c_1^{l\,2}\, dx / \int_{-\infty}^{+\infty} c_1^l\, dx \quad (19)$$

Substituting eq 18 into eq 19 and integrating, we obtain

$$\bar{c}_1^{l}(t) = \frac{lV_{inj}V_r}{v_1^{l}w_2v_2\sigma V_{tot}(2\pi)^{1/2}} \quad (20)$$

In the next step, averaging over time will yield the average value c_1^{l*} to be used as a characteristic concentration when considering the influence of the thermodynamic interaction parameters on the retention time

$$c_1^{l*} = \int_0^{t_p} \bar{c}_1^{l}(t)\, dt/t_p \quad (21)$$

Substituting the time-dependent value of σ from eq 12 (in which an equality $x_{max}/l = t/t_p$ is used) into eq 20 and using the result as integrand in eq 21, we obtain

$$c_1^{l*} = \frac{2lV_{inj}V_r}{v_1^{l}w_2v_2V_{tot}\sigma_o(2\pi)^{1/2}(1 + \sigma_i/\sigma_o)} \quad (22)$$

Combination of eq 22 with eq 13 simplifies the result to

$$c_1^{l*} = \frac{4(\ln 2)^{1/2}V_{inj}V_g}{v_1^{l}v_2V_{h/2}(2\pi)^{1/2}(1 + \sigma_i/\sigma_o)} \quad (23)$$

where the specific retention volume V_g was defined as usually as $V_g \equiv V_r/w_2$.

Finally, the dependence of the retention volume on the injected volume of probe is obtained by substituting c_1^{l*} from eq 23 for c_1^{l} in eq 11. The result reads

$$V_r \approx V_r^* + \frac{4(2 \ln (2/\pi))^{1/2}(1 + \chi)}{v_2(1 + \sigma_i/\sigma_o)} \frac{V_gV_r^*}{V_{h/2}} V_{inj} \quad (24)$$

Thus V_r is a linear function of the volume of the injected probe V_{inj}; the slope is given by the coefficient of V_{inj} in the second term on the right side of eq 24. For a given polymer–solvent pair at a given temperature, the ratio $V_r^*/V_{h/2}$ varies only slowly with the flow rate of the carrier gas and with the column loading. It follows that the dependences of V_r on V_{inj} for different flow rates and different loadings will have similar slopes. However, V_r^* is proportional to column loading: the relative contribution of the second term of eq 24 increases with decreasing loading and so does its significance for calculation of the values of V_g. When different probes and/or temperatures are studied under comparable conditions, the significance of the dependence on injected volume increases with increasing value of V_g, i.e., with increasing polymer–probe interaction.

Experimental Section

Apparatus and Procedures. Measurements were made on a modified Varian Aerograph Model 2100-40 gas chromatograph equipped with a flame ionization detector. The modifications made to this instrument and the method of coating the polymer have been reported previously.[1] We have further modified the instrument and redesigned the plumbing system to reduce the dead volume: the symmetry of the peaks improved considerably.

Dried helium was used as a carrier gas; methane served as a marker. The flow rate was controlled by a thermostated precision needle valve and measured by a soap-bubble flow meter. We have found that helium diffuses through the soap bubble, causing apparent reduction of the flow rate (and consequently of apparent retention volumes) by almost 10% at the lowest flow rate (4 mL/min). We have reported the description, analysis, and correction for the erroneous flow rate measurements elsewhere.[2] To improve further the internal consistency of our data, we have measured the void volume V_0 of each column by measuring the retention time of the marker at several flow rates using both helium and nitrogen as carrier gases. Correction for soap-bubble diffusion was applied for helium; no correction was needed for nitrogen. All values of the void volume were the same within ±1%. The average value of V_0 served then as a reference for measurement of flow rates and retention volumes. Thus, V_{tot} and $V_{h/2}$ were calculated as

$$V_{tot} = V_r + V_0 = V_0t_p/t_m \quad (25)$$

$$V_{h/2} = V_0t_{h/2}/t_m \quad (26)$$

where $t_{h/2}$ was width of the peak at half-height measured in time units.

Table I
PIB-Coated Chromatographic Columns

column	length, cm	wt of support, g	w_2, g	loading wt, %	V_0, mL
I	150	8.0040	0.00	0.0	28.56
II	150	7.9760	0.2294	2.9	27.55
III	150	7.7980	0.5139	6.6	27.57
IV	150	7.8087	1.0084	12.9	26.57

The IGC experiments were monitored with a Varian CDS III integrator in conjunction with a Hewlett-Packard dual-channel strip chart recorder. The positions of peak maxima measured by both instruments agreed within the precision of visual reading of the chart. The peak widths were read off the chart.

As we have mentioned in our previous study,[3] the flame ionization detector starts displaying nonlinearity at some (relatively small) injection volume of the probe: the onset of nonlinearity comes at lower injections when the time t_p decreases—due to either increased flow rate or decreased retention of the probe. When the summit of the peak is in the nonlinear region, its time coordinate is still recorded correctly; however, the apparent width of the peak is larger than the true width; i.e., the true width cannot be measured.

The probes were injected onto the column with a 1-μL Hamilton syringe. The injected amount was varied systematically between 0.01 and 1.0 μL. The peak areas were reasonably well correlated to the injected volumes up to the deviation point (onset of the nonlinear response of the detector). Up to the deviation point the width of the peaks was virtually independent of the injected volume: an average over this region was used in subsequent calculations (Table II). The retention times t_m and t_p used in our calculations were those recorded by the integrator.

Materials. Our polyisobutylene (PIB) sample had an intrinsic viscosity in cyclohexane at 20 °C of $[\eta]$ = 195 mL/g, corresponding to M = 379 000.

Four columns with different PIB loadings were prepared with Chromosorb W (acid washed, treated with dimethyldichlorosilane) as a solid support. Table I shows the description of these columns. The coated support was packed under vacuum into $^1/_4$-in. o.d. copper tubing that had been previously washed with methanol and then annealed. These columns were conditioned for 24 h above 80 °C prior to use. Chromatographically pure alkane probes were purchased from known sources and were checked for purity by gas chromatography prior to use.

Three sets of measurements were performed with different probes: hexane at 60 °C, octane at 60 °C, and nonane at 100 °C. Within each set of measurements, all four columns were measured in conjunction with three flow rates (in the case of nonane, columns II and IV were measured with only the middle flow rate). The three flow rates (normalized to the temperature of the column) were approximately 9, 18, and 25 mL/min. For each probe on each column at each flow rate, the dependence of V_r on injection volume was measured with 10–15 injections between 0.01 and 1.0 μL.

Results and Discussion

The experimental results are presented in Figures 1–3 as dependence of V_r on V_{inj}. For hexane, the dependences have slopes that are comparable to experimental error. However, the dependences for octane and nonane exhibit good linearity and significant positive slopes.

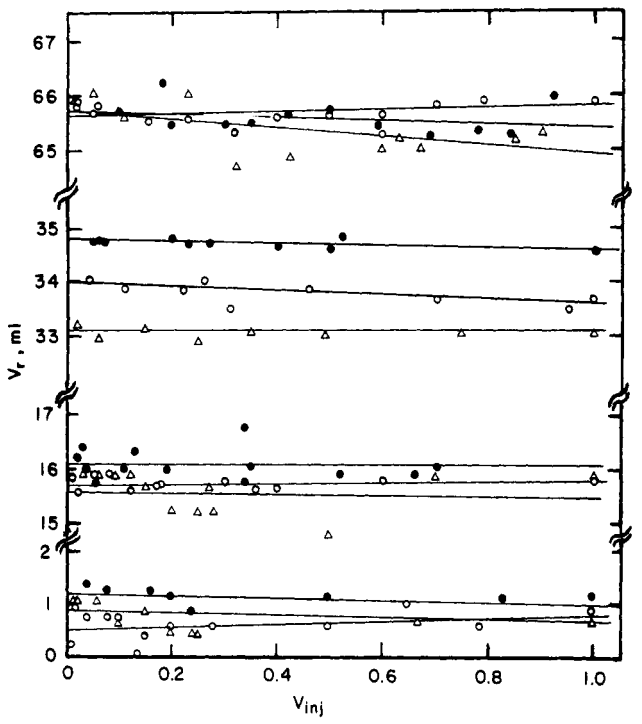

Figure 1. Dependence of retention volume on injected amount of hexane at 60 °C for columns I, II, III, and IV (from bottom to top). Flow rates (see Table IIa): (●) low; (○) medium; (△) high.

Table II
Values of V_r^*, S, $V_{h/2}$, and σ_i/σ_o for Alkane Probes on PIB Columns at Different Loadings and Flow Rates

column	F, mL/min	V_r^*, mL	$S \times 10^3$	$V_{h/2}$, mL	σ_i/σ_o
		a. Hexane at 60 °C			
I	8.7	1.2	−0.2	4.5	0.46
	18.1	0.5	0.3	3.3	0.44
	23.4	0.9	−0.4	2.8	0.46
II	8.8	16.1	0.0	6.7	0.31
	16.6	15.7	0.1	5.6	0.27
	25.2	15.6	−0.1	5.4	0.24
III	8.9	34.8	−0.2	9.8	0.21
	19.5	34.0	−0.4	8.9	0.16
	24.7	33.1	0.0	8.5	0.15
IV	8.6	65.7	−0.3	15.1	0.14
	17.8	65.6	0.2	14.5	0.10
	24.1	65.7	−0.8	15.1	0.09
		b. Octane at 60 °C			
I	8.7	5.2	1.4	4.7	0.44
	18.1	4.7	2.3	3.5	0.42
	23.4	4.8	2.5	3.0	0.44
II	8.8	100.1	9.6	18.0	0.12
	16.3	99.0	10.9	14.6	0.10
	25.2	98.4	11.1	13.4	0.09
III	8.8	215.9	11.6	34.2	0.06
	19.6	212.8	14.6	27.0	0.05
	24.7	208.5	16.0	26.4	0.05
IV	8.6	413.1	9.7	63.9	0.03
	17.8	406.2	18.2	49.6	0.03
	24.3	405.6	10.6	46.1	0.03
		c. Nonane at 100 °C			
I	10.2	2.6	0.2	4.4	0.44
	20.5	2.5	0.0	3.0	0.47
	27.6	2.3	0.2	2.6	0.47
II	21.6	54.9	5.5	8.1	0.17
III	10.2	111.8	5.1	18.4	0.10
	20.0	111.4	6.4	12.8	0.11
	27.9	112.3	6.1	11.9	0.10
IV	20.4	209.8	7.5	22.3	0.06

The experimental data were subjected to statistical analysis assuming linear dependence of V_r on V_{inj}. The

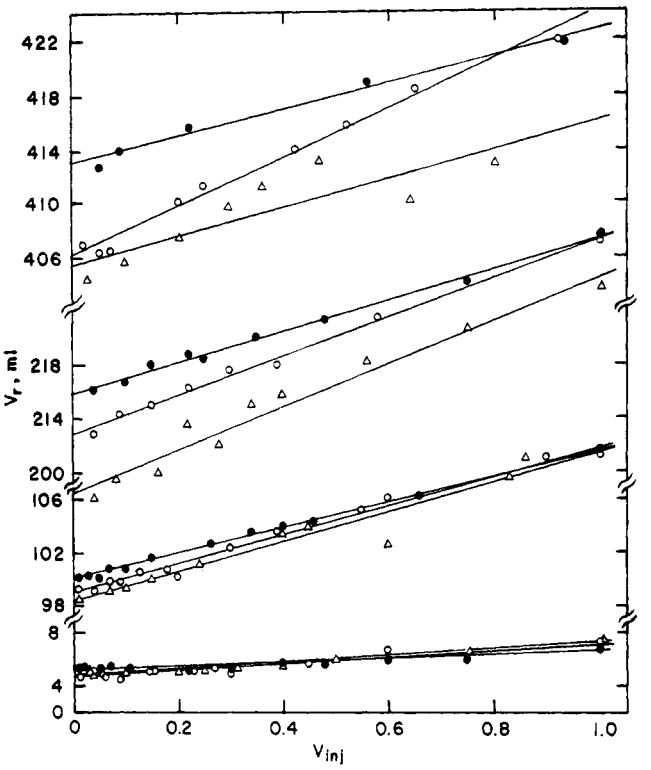

Figure 2. Dependence of retention volume on injected amount of octane at 60 °C for columns I, II, III, and IV (from bottom to top). Flow rates (see Table IIb): (●) low; (○) medium; (△) high.

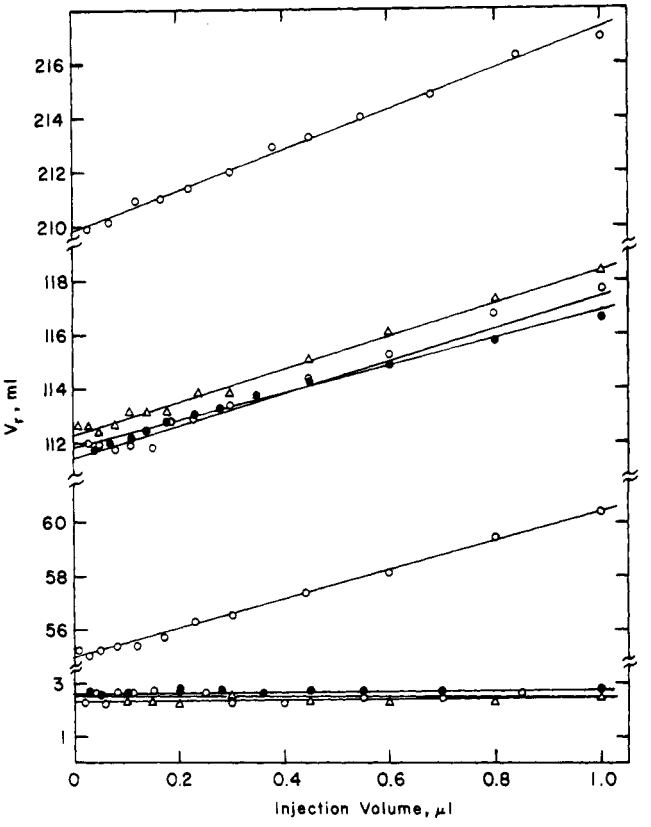

Figure 3. Dependence of retention volume on injected amount of nonane at 100 °C for columns I, II, III, and IV (from bottom to top). Flow rates (see Table IIC): (●) low; (○) medium; (△) high.

intercepts (V_r^* values) and the slopes S are collected in Table II together with values of $V_{h/2}$ and σ_i/σ_o. The latter ratio is approximated by the ratio $V_{h/2}{}^i/V_{h/2}$ where the initial half-width $V_{h/2}{}^i$ was obtained from study of the peak

Table III
Analysis of Retention Data from Table II

column	F, mL/min	V_r^*/w_2, mL/g	$(V_r^* - V_r^{0*})/w_2$, mL/g	$S \times 10^3$	$(S - S^0) \times 10^3$	$S_{th} \times 10^3$
			a. Hexane at 60 °C			
II	8.8	70.2	64.9	0.0	0.2	0.4
	16.6	68.4	66.3	0.1	−0.2	0.5
	25.2	68.0	64.1	−0.1	0.3	0.6
III	8.9	67.7	65.4	−0.2	0.0	0.7
	19.5	66.2	65.2	−0.4	−0.7	0.8
	24.7	64.4	62.7	0.0	0.4	0.8
IV	8.6	65.2	64.0	−0.3	−0.1	0.9
	17.8	65.1	64.6	0.2	−0.1	1.0
	24.1	65.2	64.3	−0.8	−0.4	0.9
			b. Octane at 60 °C			
II	8.8	436.4	413.7	9.6	8.2	7.0
	16.3	431.6	411.1	10.9	8.6	8.7
	25.2	429.0	408.0	11.1	8.6	9.5
III	8.8	420.1	410.0	11.6	10.4	8.4
	19.6	414.1	404.9	14.6	12.3	10.6
	24.7	405.7	396.4	16.0	13.5	10.6
IV	8.6	409.7	404.5	9.7	8.3	8.9
	17.8	402.8	398.2	18.2	15.9	11.2
	24.3	402.2	397.5	10.6	8.1	12.1
			c. Nonane at 100 °C			
II	21.6	239.3	228.4	5.5	5.5	4.1
III	10.2	217.6	212.5	5.1	4.9	4.0
	20.0	216.8	211.9	6.4	6.4	5.6
	27.9	218.5	214.1	6.1	5.9	6.2
IV	20.4	208.1	205.8	7.5	7.5	6.4

spreading in the plumbing of the column.[12]

The extrapolated retention volumes V_r^* measured for the same probe on the same column at different flow rates differed not more than ±0.5 mL for small retention volumes and ±2% (in the worst case) for large retention volumes. We consider these errors to be representative for the overall precision of our IGC measurements. We have shown in our previous communication that a proper evaluation of the retention data requires subtraction of the retention of the uncoated support from the retention of the column coated by polymer. This procedure totally eliminated the apparent dramatic increase of the retention volume at very small injections of polar probes and led to values of specific retention volumes V_g that were essentially independent of the column loading. Accordingly, we are presenting in Table II two sets of values of V_g: values uncorrected for the retention of the support V_r^*/w_2 and values corrected for it $(V_r^* - V_r^{0*})/w_2$. Here V_r^{0*} refers to retention volumes measured on our uncoated column I. The corrected data for hexane at 60 °C are independent of column loading; i.e., the differences among columns are not larger than the differences of values measured on the same column at different flow rates. For octane at 60 °C the uncorrected V_g values increase with decreasing loading: the difference between columns II and IV is about 7%. The correction for the retention by support reduces this difference to about 3%; that is slightly more than our experimental error. However, for nonane at 100 °C, the difference for the uncorrected data is about 15%. It is reduced to about 11% for the corrected data; that is far above the experimental error. Thus, it seems that the dependence of V_g on column loading is real; it is small under some circumstances and significant at other conditions. We plan to study this dependence in detail in our continuing research.

The experimental and theoretical values of the slopes S are compared in Table III. The experimental values are given as uncorrected ones (S) and corrected ones ($S - S^0$), where S^0 is the slope measured on the uncoated column at an appropriate flow rate. The theoretical values of the slope S_{th} were calculated as the values of the coefficient of the last term in eq 24 using the experimental values V_r^*, $V_{h/2}$, and σ_i/σ_o. For the specific volume of polyisobutylene v_2, the value of 1.118 mL/g was used at 60 °C and 1.145 mL/g was used at 100 °C. The same value of V_g was used for all columns and flow rates; it was the average value of $(V_r^* - V_r^{0*})/w_2$ from Table III. The average was 64.6 mL/g for hexane, 404.9 mL/g for octane, and 214.5 mL/g for nonane. The values of the parameter χ were obtained from eq 9 and appropriate auxiliary data: χ was equal to 0.55 for hexane, 0.47 for octane, and 0.41 for nonane. (Newman and Prausnitz[9] observed for hexane χ equal to 0.58 at 50 °C and 0.57 at 75 °C.)

Before comparing the experimental and theoretical values of the slope, we should realize that a value $S \times 10^{-3} = 1.0$ represents an increase of 1 mL of the value of V_r when going from vanishing injection to our maximum injection of 1 μL. This increase is well within our experimental error. Thus, our theory predicts that for hexane at 60 °C the slope should be negligible; this was indeed observed experimentally. For octane at 60 °C and nonane at 100 °C, the agreement between experimental and theoretical values is remarkably good. The difference between $(S - S^0)$ and S_{th} is larger than 2.0×10^{-3} for only three dependences out of 23 measured.

Conclusions

The theoretical treatment of the dependence of the retention volume of a probe on the amount injected describes the experimental dependences quite satisfactorily. The agreement is remarkable considering that the theory does not contain any adjustable parameter.

The main significance of the theory is in the fact that it allows an estimate of the slope from a single IGC experiment, which provides all the relevant values: V_r, V_g and $V_{h/2}$. From the slope and the known volume of injection, the correction for nonvanishing injection may be computed. For example, slope $S \times 10^{-3} = 10.0$ and $V_{inj} = 0.05$ μL suggest a correction of V_r by 0.5 mL. This correction may have some significance when V_r values are small. The correction becomes more significant when the chromatographic peaks become very broad, e.g., due to

very small flow rates. In such a situation, a large amount of probe is usually injected to improve the signal-to-noise ratio of the detector: then the correction gets larger because V_{inj} is large. The correction is also significant for very small column loadings. As is seen from Figures 1–3 and tables, the slopes for different loadings are very similar due to the fact that V_r and $V_{h/2}$ are more or less proportional to each other. Thus, the correction of V_r is similar for different loadings; for small loadings (small V_r) its relative significance increases.

Acknowledgment. We are grateful to Hercules, Inc., for financial support of this study through its Grant-in-Aid program.

Registry No. Poly(isobutylene), 9003-29-6; hexane, 110-54-3; octane, 111-65-9; nonane, 111-84-2.

References and Notes

(1) Al-Saigh, Z. Y.; Munk, P. *Macromolecules* **1984**, *17*, 803.
(2) Card, T.; Al-Saigh, Z. Y.; Munk, P. *J. Chromatogr.* **1984**, *301*, 261.
(3) Card, T.; Al-Saigh, Z. Y.; Munk, P. *Macromolecules* **1985**, *18*, 1030.
(4) Leung, Y.-K.; Eichinger, B. E. *J. Phys. Chem.* **1974**, *78*, 60.
(5) Leung, Y.-K.; Eichinger, B. E. *Macromolecules* **1974**, *7*, 685.
(6) Hammers, W. E.; Deligny, C. L. *Recl. Trav. Chim. Pays-Bas* **1971**, *90*, 912; *J. Polym. Sci., Part C* **1972**, *39*, 273.
(7) Newman, R. D.; Prausnitz, J. M. *J. Phys. Chem.* **1972**, *76*, 1492.
(8) Lichtenthaler, R. N.; Liu, D. D.; Prausnitz, J. M. *Macromolecules* **1974**, *7*, 565.
(9) Newman, R. D.; Prausnitz, J. M. *AIChE J.* **1973**, *19*, 704.
(10) Braun, J. M.; Guillet, J. E. *Macromolecules* **1975**, *8*, 557.
(11) Fernandez-Berridi, M. J.; Eguiazabal, J. I.; Elorza, J. M. *J. Polym. Sci., Polym. Phys. Ed.* **1983**, *21*, 859.
(12) Munk, P.; Al-Saigh, Z. Y.; Card, T., paper in preparation.

Dual-Mode Transport of Penetrants in Glassy Polymers

Glenn H. Fredrickson* and Eugene Helfand

AT&T Bell Laboratories, Murray Hill, New Jersey 07974. *Received April 22, 1985*

ABSTRACT: The existing theories of dual-mode penetrant transport in amorphous polymers are critically examined. It is found that terms in the penetrant flux expression that couple the two sorption modes have previously been neglected. The importance of these terms is discussed, and new expressions for the time lag and permeability in permeation experiments are presented. Our theory reduces to previous theories by Paul and Koros and by Petropoulos in particular limits, but the interpretation of certain parameters in these theories is modified.

I. Introduction

An understanding of penetrant sorption and diffusion in polymers is essential to many industrial applications. Polymer films and membranes are used extensively in food packaging, industrial gas separation processes, drug delivery systems, and reverse osmotic applications. The design of effective coating and casings for the protection of electronic components and transmission cables depends critically on the sorption properties of undesirable penetrants in the protective coatings. A successful theory of sorption and transport can also be applied to the analysis of dye penetration and binding in textiles and to membranes that contain adsorptive fillers for applications demanding controlled penetrant transport.

While the solubility and transport properties of small molecules in rubbery polymers are relatively well understood, much less is known about the microscopic mechanism of sorption and transport in glassy polymers. It is believed that the inability of the sub-T_g matrix to relax to thermodynamic equilibrium can lead to local inhomogeneities in the penetrant environment. Furthermore, gas absorption by polymeric glasses can be accompanied by swelling, crazing, and crack formation. There are several excellent reviews of theory and experiment for penetrant solubility and mobility in glassy systems.[1-3]

Meares[4] was one of the first to suggest that the inhomogeneities present in polymer glasses have a profound effect on penetrant solubility and transport. He proposed a "dual-mode" picture in which penetrant molecules can reside in one of two environments in the glass. The first environment (or "mode") is that of ordinary solution, while in the second mode penetrant molecules reside in "microvoids" or holes that were frozen into the glass at T_g. Vieth, Michaels, and Barrie[5,6] demonstrated that various inert gases show highly nonlinear sorption isotherms in glassy polymers. They found that these isotherms could be empirically represented as a sum of a Henry's law contribution and a Langmuir contribution

$$C = C_D + C_H = k_D p + C_H' bp/(1 + bp) \qquad (1)$$

where C is the total concentration of penetrant, C_D is the concentration of "dissolved" molecules, C_H is the concentration of molecules "adsorbed in microvoids," k_D is Henry's law constant, b is the hole affinity constant, C_H' is the concentration in the holes at saturation, and p is the partial pressure of penetrant in the gas phase. The applicability of eq 1 to a wide variety of penetrants and polymers has been demonstrated.[2]

A description of the kinetics of permeation was first given by Vieth and Sladek,[7] who proposed that the molecules in the microvoids are completely immobilized. Petropoulos[8] and Paul and Koros[9] subsequently extended the transport theory to allow partial mobility of the adsorbed penetrant molecules. Tshudy and von Frankenberg[10] also generalized the Vieth–Sladek analysis by relaxing the assumption of local equilibrium. The combination of eq 1 and these transport models is collectively referred to as dual-mode sorption theory. There is increasing evidence[1-11] that the dual-mode description is a realistic picture of sorption and transport for nonswelling penetrants in glassy polymers.

Despite the success of the dual-mode transport theories, there are some unsatisfactory steps and assumptions in the derivation of the working equations. Furthermore, the existing derivations[8,9] leave unanswered questions regarding the physical interpretation of certain transport parameters and the origin of penetrant mobility in the microvoids. The objective of this paper is to clarify some

0024-9297/85/2218-2201$01.50/0